Self-assembled InGaN Quantum Dots Grown by Molecular Beam Epitaxy

MBE 法による InGaN 自己形成量子ドット

T.M. Smeeton* K.L. Smith* M. Senes* S.E. Hooper* J. Heffernan*

Abstract

InGaN-based semiconductor optoelectronic devices have significant applications in Blu-ray optical storage and solid-state lighting. Improvements in the performance of these devices are expected if InGaN quantum dot active regions are used in place of the quantum wells which are currently used. In this paper we report the growth of InGaN quantum dots by molecular beam epitaxy (MBE) at Sharp Laboratories of Europe. The structures contain a high density (1.5×10^{11} cm^{-2}) of $In_{0.15}Ga_{0.85}N$ quantum dots which are formed by self-organised nano-island growth and have typical diameters of 10 nm and heights of 1.7 nm. The quantum dots exhibit photoluminescence at blue/violet wavelengths of ~430 nm and micro-photoluminescence measurements are used to reveal light emission from discrete energy states in individual dots. The quantum dot properties suggest that they are well suited for use in the active regions of visible-wavelength optoelectronic devices.

InGaN系半導体を用いた発光デバイスは，次世代DVDブルーレイや固体照明用光源として重要である。このとき，通常活性層として利用されている量子井戸にかえてInGaN量子ドットを用いることができれば，デバイスの性能は飛躍的に向上すると期待されている。本稿では，MBE （分子線エピタキシー） 法によるInGaN量子ドットの成長に関するシャープヨーロッパ研究所の取り組みについて述べる。自己形成ナノアイランド成長法によって形成した$In_{0.15}Ga_{0.85}N$量子ドットは，1.5×10^{11} cm^{-2}と高密度であり，そのサイズはおよそ直径10 nm高さ1.7 nmである。この量子ドットは波長約430 nmの青紫色のフォトルミネッセンスを示し，これは個々のドットの不連続なエネルギー準位からの発光であることが，顕微フォトルミネッセンスを用いた評価により確認された。このことは，この方法によって作成した量子ドットが可視光領域の発光デバイスの活性層として利用するに十分な特性を有していることを示している。

Introduction

Optoelectronic devices based on the group III-nitride semiconductor compounds GaN, $In_xGa_{1-x}N$ and $Al_yGa_{1-y}N$ are essential for the important and expanding businesses of solid-state lighting and Blu-ray optical storage. Virtually all examples of the blue-violet laser diodes used in Blu-ray systems and the high-brightness blue, green and white light emitting diodes (LEDs) required for the impending solid-state lighting revolution use active regions containing InGaN quantum wells [e.g. 1].

An alternative technology for future generations of III-nitride optoelectronic devices is the use of active regions containing InGaN quantum dots. Whereas a quantum well is an electron and hole confining layer which is thin enough (typically less than a few tens of nanometres) in one dimension that the behaviour of the

*Sharp Laboratories of Europe Ltd.

carriers is significantly affected by quantum size effects, a quantum dot is as small as this in all three dimensions. The three-dimensional quantum size effects cause the energy states for electrons and holes to be quantised into discrete levels which are similar to those in atoms. This "artificial atom" behaviour gives quantum dots several theoretical advantages over quantum wells in optoelectronic device applications [2]. III-nitride quantum dots have also been recommended for use in many other devices which offer entirely new functionality, such as providing an effective medium for exploiting electron spin effects and providing a viable platform for quantum information processing [3].

Amongst optoelectronic devices, laser diodes in particular benefit from huge potential improvements associated with the use of quantum dots instead of quantum wells. The theoretical advantages include lower threshold currents (and therefore lower power consumption) due to the concentration of electrons and holes into discrete states in a very narrow energy range, and temperature-insensitive threshold currents, due to the large energy differences between the discrete states [4; 5]. These important improvements, and several others, have been demonstrated for In(Ga)As-based laser diodes [e.g. 5] and there is a growing commercial interest in this technology for optical telecommunication applications [e.g. 6].

The predicted advantages for quantum dots in III-nitride lasers are in principle much more significant than for III-arsenide devices, especially in relation to reductions in threshold current density [7]. Although it is well known that many InGaN "quantum wells" exhibit exciton localisation effects similar to those expected in quantum dot systems [e.g. 8], genuine quantum dot structures - analogous to those successfully used in III-arsenide materials - will allow the quantum dot properties to be fully exploited. The successful realisation of these quantum dot structures represents the next, and possibly final, stage of the reduction in the dimensions and dimensionality of III-nitride device active regions which has taken place over the past decade.

In III-arsenide materials the most successful method of forming quantum dots suitable for use in device active regions has been based on exploiting the self-organised growth of epitaxial nano-islands. This self-assembly approach is compatible with existing epitaxial growth methods and conventional planar device structures. The spontaneous formation of nano-islands has been widely studied since the mid-1980s and shown to deliver inclusions with are free of extended crystalline defects such as dislocations and behave as quantum dots [e.g. 2].

Similar results for InGaN nano-island growth [9-12] are less extensive but demonstrate the potential of this approach for III-nitride materials. Self-organised InGaN nano-islands have been grown using metalorganic vapour phase epitaxy (MOVPE) [9] and shown to exhibit quantum dot behaviour [13]. InGaN nano-islands have also been prepared using the alternative growth technique of molecular beam epitaxy (MBE) [10-12], which benefits from compatibility with powerful in-situ characterisation tools such as reflection high-energy electron diffraction (RHEED) which can be used to study the formation of nano-islands in real time [14]. Luminescence analysis of these samples also indicated behaviour distinct from that typical of InGaN quantum wells at the time [10, 11] but neither the combined measurement of detailed structural and optical properties of the samples, nor the application of the structures in electroluminescent devices was reported.

In this paper we describe InGaN quantum dot active regions grown at Sharp Laboratories of Europe. The structures were grown using MBE, building on the technology developed during this laboratory's recent demonstration of the world's first continuous wave III-nitride laser diode grown by MBE [15]. We present structural and optical characterisation results which prove the samples contain quantum dots (i.e. InGaN inclusions which exhibit three-dimensional quantum size effects) and suggest that they are well suited to application in electroluminescent devices.

1. Experimental details

The samples were grown by MBE on commercially available n-type (0001) GaN-on-sapphire templates [16] in a SVT Associates MBE system. Elemental effusion cells were used as sources of gallium, aluminium, indium and silicon. Sample A consisted of a 250 nm GaN:Si n-type buffer layer, a 20 nm $Al_{0.1}Ga_{0.9}N$ layer, a 100 nm GaN layer and finally an InGaN quantum dot layer. With the exception of the InGaN layer, this material was grown using ammonia (NH_3) thermally cracked at the substrate surface as the nitrogen source. The InGaN layer was grown under nitrogen-excess conditions using activated nitrogen generated from a radio-frequency plasma cell (Veeco Unibulb). Immediately after growth the layer was subjected to a two minute interruption at the growth temperature and in the presence of the activated nitrogen flux before being

rapidly cooled to room temperature for ex-situ analysis. No changes were observed in the RHEED pattern during the rapid cooling of the sample so we assume that there were no significant alterations to the sample morphology during this process. Sample B was exactly the same as sample A, except for the overgrowth of a 15 nm GaN cap using the activated nitrogen immediately after the post-InGaN-growth interrupt.

In-situ RHEED patterns were recorded from the substrate surface during growth using a digital video camera focussed on a phosphor screen and subsequently analysed off-line. Atomic force microscopy (AFM) height images were obtained using a DI Dimension 3100 scanning probe microscope in tapping mode with silicon cantilevers and fresh tips with nominal radii of curvature of less than 10 nm. Wedge-shaped specimens suitable for transmission electron microscopy analysis were prepared by mechanical thinning using diamond lapping films and final thinning using an ion miller (Gatan PIPS; 3.5 keV argon ions). High-resolution TEM and Z-contrast (high-angle annular dark field) scanning TEM results were acquired along <11$\bar{2}$0> directions using an FEI Tecnai F20 G2 (S)TEM with a Schottky field emission source operating at 200 keV. Care was taken to minimise the electron irradiation of the specimens to avoid artefacts caused by the sensitivity of thin InGaN layers to electron beam damage [17].

The optical properties of the samples were compared with those of an InGaN quantum well with GaN barriers.

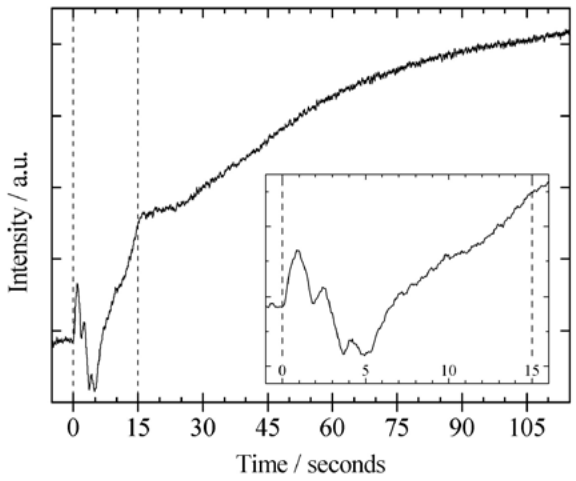

Fig. 1 The RHEED specular intensity during the InGaN growth and post-growth interrupt for sample A. The vertical dashed lines correspond to the start and end of the growth period and the inset shows the initial time range in more detail.

This quantum well sample was grown by MBE using ammonia as the source of nitrogen and exhibited a room temperature photoluminescence (PL) peak centred at 420 nm. The composition and thickness of the quantum well and the thickness of the GaN cap were determined to be $In_{0.13}Ga_{0.87}N$, 2.5 ± 0.3 nm and 16 ± 1 nm respectively using high-resolution X-ray diffraction and high-resolution transmission electron microscopy.

Time-integrated PL measurements were recorded using an excitation wavelength of 325 nm (HeCd laser) and a 0.8 m double spectrometer coupled to a photomultiplier tube. Micro-PL measurements were recorded from small circular apertures (170 nm diameter) which were opened in a 100 nm thick evaporated aluminium mask using electron beam lithography and wet chemical etching. The micro-PL spectra were measured using a Renishaw inVia reflex confocal microscope in which the laser beam (325 nm; HeCd laser) was focussed to a diameter of ~5 μm at the sample surface. The sample was mounted in a helium flow cryostat that was cooled to 4 K, and the luminescence was recorded using a charge coupled device (CCD) after dispersion on a 50 cm monochromator with 1800 grooves mm^{-1}. The best spectral resolution of this system is approximately 1.8 meV.

2. Results & discussion

i) Quantum dot growth and structure

The variation of the RHEED pattern during the InGaN growth and post-growth interrupt of sample A illustrates the formation of surface nano-islands in our samples. Fig. 1 shows the evolution of the RHEED pattern intensity as a function of time, monitored at a position coinciding with the tail of the specular streak in the pattern of the flat starting surface. The periodic intensity oscillations which

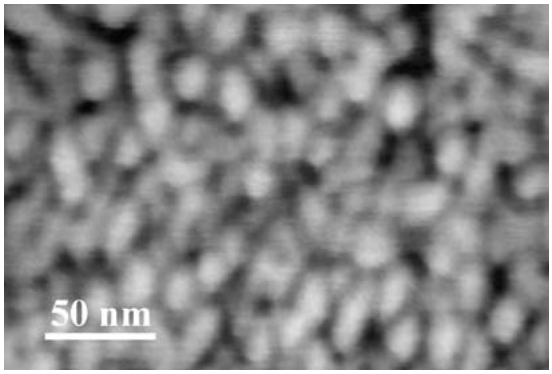

Fig. 2 An AFM height image of sample A (greyscale height range is 3 nm).

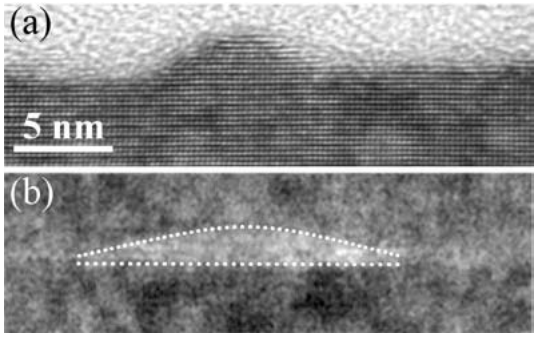

Fig. 3 (a) A HRTEM image of an InGaN nano-island in sample A;
(b) A Z-contrast image of an InGaN inclusion in sample B. The higher intensity in the Z-contrast image corresponds to a higher indium fraction. The dashed lines indicate the approximate boundary between the InGaN and the GaN matrix. The scale bar applies to both images.

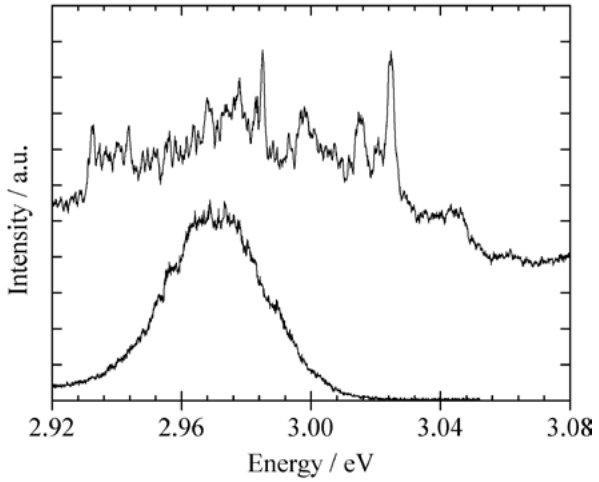

Fig. 4 Micro-PL spectra acquired at 4 K from 170nm diameter regions of sample B (top line) and the quantum well sample (bottom line).

were exhibited during the first five seconds of InGaN growth are characteristic of layer-by-layer two dimensional growth [e.g. 14] with a growth rate of 0.6 monolayers per second (one monolayer corresponds to half the *c* lattice parameter of the wurtzite crystal).

The cessation of the oscillations after five seconds coincided with a change in the RHEED pattern from one containing streaks to one composed of spots. This is indicative of a transition from electron reflection from a flat growth surface to electron diffraction through three-dimensional asperities on the growth surface. This suggests that once the deposited thickness exceeded about three monolayers the growth proceeded in a three-dimensional island-growth mode. The strengthening of the spot intensity during the remainder of the InGaN growth period and also during the interrupt, which is indicated by the continuous increase in intensity plotted in Fig. 1, may signify a coarsening of the islands. An AFM height image of sample A is shown in Fig. 2. This shows that after the InGaN growth and interrupt the morphology was dominated by closely-spaced surface nano-islands with a high density of $\sim 1.5 \times 10^{11}$ cm^{-2}.

A cross-sectional HRTEM image of a typical surface island is shown in Fig. 3 (a). Analysis of HRTEM images of several islands revealed that most had a base diameter of (10 ± 4) nm and a height (measured relative to the valley minimum in between islands) of (1.7 ± 1.0) nm. There is very weak contrast between the GaN and InGaN in the image (because the TEM specimen was relatively thin) so it is not possible to identify the position of the interface between the two materials. This means that we cannot determine from this data whether the InGaN islands were connected by a continuous "wetting layer" or were isolated from one another on the GaN underlayer. The absence of any strong contrast at the interface, and the continuity of the phase contrast image intensity maxima (the "atomic columns") across it, are consistent with the interface being coherent and this suggests that the nano-islands are dislocation-free. The stacking sequence of (0001) monolayers inferred from the HRTEM images indicated that the islands had the wurtzite structure.

During overgrowth of the InGaN islands with GaN (sample B), the RHEED pattern rapidly underwent a transition from spotty to streaky. This indicates that the growth surface rapidly returned to a planar morphology and AFM height images of the cap (not shown) showed that this was the case. Cross-sectional scanning TEM Z-contrast imaging of this sample revealed InGaN inclusions with a size distribution similar to that of the uncapped InGaN islands. This shows that the islands were preserved during the capping and that their sizes were not substantially altered during the GaN overgrowth. A typical Z-contrast image of an InGaN inclusion is shown in Fig. 3 (b). The difference in shape between the uncapped island in Fig. 3 (a) and the capped inclusion in Fig. 3 (b) reflects the size distribution in the sample and does not represent a systematic change in island shape caused by GaN overgrowth. The indium fraction of the InGaN inclusions was estimated from the ratio of the electron scattering

to the high-angle annular detector from InGaN and GaN regions. This indicated a composition of $In_{0.15}Ga_{0.85}N$, assuming that the high-angle scattering was proportional to Z^2 (Z is the atomic number), and assuming that the InGaN inclusions occupied the entire thickness of the TEM specimen.

ii) Quantum dot optical properties

Clear evidence that the InGaN inclusions in sample B are quantum dots is obtained from micro-PL measurements of very small portions of the InGaN layer. A spectrum acquired from a region of the sample which contained less than fifty InGaN inclusions (assuming a density of 1.5 × $10^{11}cm^{-2}$) is plotted in Fig. 4 and it shows that narrow emission lines can be identified in the luminescence. This behaviour is similar to that reported for luminescence from InGaN quantum dot structures grown by MOVPE [13, 18]. The narrowest lines in the spectrum have full-widths at half maxima (FWHM) equal to (and therefore possibility limited by) the spectral resolution of the spectrometer. These narrow emission lines are characteristic of luminescence from localised states with discrete energy levels and therefore this result provides direct evidence of three-dimensional quantum size effects in sample B. The micro-PL spectrum from a similarly small portion of the quantum well sample, which is also plotted in Fig. 4, shows entirely different behaviour: the luminescence consists of a continuous spectrum with no narrow lines (the loose structure and spikes in this spectrum are due to Fabry-Pérot interference effects and statistical noise). This spectrum reflects the continuous density of states of the quantum well with no measurable emission from discrete energy levels. The two spectra plotted in Fig. 4 are characteristic of many acquired from different regions of sample B and the quantum well sample. The presence of narrow luminescence lines in the sample B spectra and the absence of these lines in the quantum well spectra illustrates an important difference between genuine nano-island-growth quantum dots and quantum wells exhibiting localisation effects.

A room-temperature PL spectrum from a large ensemble of quantum dots in sample B (~10^6 quantum dots, assuming a density of 1.5 × $10^{11}cm^{-2}$) is plotted in Fig. 5. This luminescence peak is centred at 430 nm (an energy of 2.89 eV) and has a FWHM of 30 nm. The peak is broader than is typical for InGaN quantum wells emitting at a similar wavelength (FWHM~15-20 nm) and this is likely to be a consequence of the dispersion in the composition

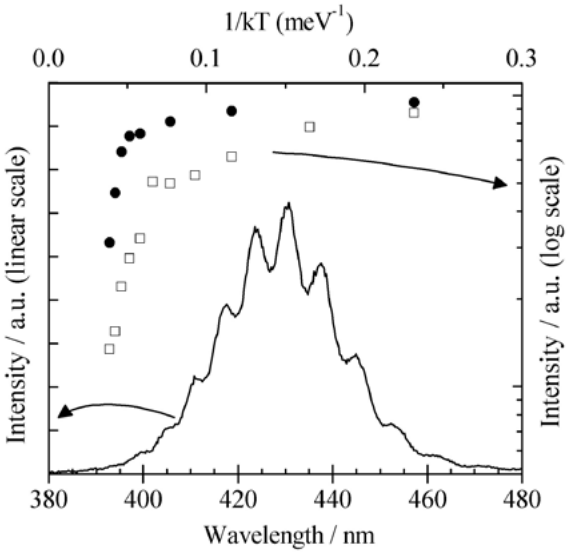

Fig. 5 Bottom/left axes: a time-integrated room-temperature PL spectrum from sample B. The oscillations in the peak intensity are caused by Fabry-Pérot interference between the directly emitted light and light reflected at the interface between the GaN epilayer and the sapphire substrate. Top/right axes: PL intensity as a function for temperature for sample B (filled circles) and the quantum well sample (open squares).

and/or size of the quantum dots which results in a range of different emission energies from the ensemble as a whole.

A striking difference between the optical properties of sample B and a typical quantum well is the variation of PL intensity with temperature. This is also plotted in Fig. 5. As the temperature of the sample is increased, the greater thermal energy activates more diffusion of the carriers to defects so the likelihood of non-radiative recombination increases and therefore the luminescence intensity falls. Fig. 5 shows that the decline in intensity is substantially smaller for the quantum dots in sample B than for the quantum well. This robustness of the quantum dot luminescence intensity to temperature increase indicates that the diffusion of carriers to non-radiative recombination centres is reduced, and therefore that the spatial localisation of carriers in the quantum dots is much stronger than in the quantum well. Due to limitations in the power of our excitation source, the data plotted in Fig. 5 were for powers substantially below those corresponding to the maximum internal radiative efficiency of the samples and therefore provide an underestimate of this parameter.

We end this paper by briefly comparing the growth, structure and optical properties of our samples with results previously reported for InGaN nano-islands. The transition from two-dimensional growth to three-dimensional growth inferred from the RHEED measurements, and the high-island density revealed by AFM results is similar to earlier reports of InGaN nano-island growth [10-12, 14]. By extending beyond the scope of earlier work to analyse the nano-islands in more detail using cross-sectional (S)TEM we have been able to attain a more accurate indication of the size and shape of both the as-grown nano-islands and the InGaN inclusions after GaN capping. Most significantly, however, for the first time we have combined these structural measurements with a clear demonstration that the InGaN exhibits three-dimensional quantum size effects - and therefore proven that the InGaN inclusions are genuine "quantum dots". The current focus of our research is to realise the advantages of these quantum dots in electroluminescent devices.

Conclusions

In summary, we have shown that InGaN quantum dot layers can be successfully grown using MBE. The samples exhibit definitive quantum dot behaviour and luminescence at blue/violet wavelengths. The results suggest that these active regions are promising candidates for use in visible wavelength optoelectronic devices which benefit from three-dimensional quantum confinement effects.

Acknowledgements

We are very grateful to Prof Colin Humphreys of the Department of Materials Science and Metallurgy at the University of Cambridge for providing access to TEM facilities.

References

[1] S. Nakamura, S. Pearton and G. Fasol, The Blue Laser Diode (2nd Ed), Springer (2000).

[2] D. Bimberg, M. Grundmann and N.N. Ledentsov, Quantum Dot Heterostructures, Wiley (1999).

[3] V.A. Shchukin, N.N. Ledentsov and D. Bimberg, Epitaxy of Nanostructures, Springer-Verlag (2003).

[4] Y. Arakawa and H. Sakaki, Appl. Phys. Lett. 40 939 (1982).

[5] D. Bimberg et al., J. Phys.: Condens. Matter 15 R1063 (2003).

[6] Optics & Laser Europe, June 2006, p21.

[7] Y. Arakawa, phys. stat. sol. (a) 188 37 (2001).

[8] S.F. Chichibu et al., Nature Materials 5 810 (2006).

[9] K. Tachibana et al., Appl. Phys. Lett. 74 383 (1999).

[10] B. Damilano et al., Appl. Phys. Lett. 75 3751 (1999).

[11] C. Adelmann et al., Appl. Phys. Lett. 76 1570 (2000).

[12] Y. Yamaguchi et al., Mater. Res. Soc. Symp. Proc. 831 69 (2005).

[13] O. Moriwaki et al., Appl. Phys. Lett. 76 2361 (2000).

[14] N. Grandjean and J. Massies, Appl. Phys. Lett. 72 1078 (1998).

[15] M. Kauer et al., Electron. Lett. 41 739 (2005) and Sharp Technical Journal 92 72 (2005).

[16] Lumilog "Standard" templates

[17] T.M. Smeeton et al., Appl. Phys. Lett. 83 5419 (2003).

[18] J.W. Robinson et al., Appl. Phys. Lett. 83 2674 (2003).

(received November 8, 2006)